"Millipede" – an AFM data storage system at the frontier of nanotribology

U. Dürig [a], G. Cross [a], M. Despont [a], U. Drechsler [a], W. Häberle [a], M.I. Lutwyche [a], H. Rothuizen [a], R. Stutz [a], R. Widmer [a], P. Vettiger [a], G.K. Binnig [a], W.P. King [b,*] and K.E. Goodson [b]

[a] *IBM Research, Zurich Research Laboratory, CH-8803 Rüschlikon, Switzerland*
[b] *Department of Mechanical Engineering, Stanford University, Stanford, CA 94305-3030, USA*

The "Millipede" data storage concept is based on the parallel operation of a large number of micromechanical levers that function as AFM sensors. The technique holds promise to evolve into a novel ultrahigh-density, terabit-capacity, and high-data-rate storage technology. Thermomechanical writing and reading in very thin polymer (PMMA) films is used to store and sense 30–40 nm sized bits of similar pitch size, resulting in 400–500 Gbit/in^2 storage densities. High data rates are achieved by operating very large arrays (32×32) of AFM sensors in parallel. Batch-fabrication of 32×32 AFM cantilever array chips has been achieved, and array reading and writing have been demonstrated. An important consideration for the Millipede storage project is the polymer dynamics on the size scale of one bit. Scaling of rheological parameters measured for macroscopic polymer samples is likely to be incorrect due to the finite length of the underlying molecular polymer chain, a size that is comparable to the bit itself. In order to shed light on these issues we performed lifetime studies of regular arrays of nanometer size patterns using light-scattering techniques.

Keywords: Millipede, atomic force microscopy, micromechanics, data storage, light scattering, polymer flow

1. Introduction

Atomic force microscopy (AFM)-based data storage is a promising alternative to conventional magnetic data storage because it offers great potential for considerable storage density improvements [1]. We have recently demonstrated storage densities of up to 500 Gbit/in^2 by thermomechanical writing and thermal readout in thin polymer films with bit sizes and pitches of 30–40 nm each [2,3]. This is about 40–50 times more than today's best research demonstrations with magnetic recording [4]. The highest data rate achieved with fast single levers is 6 Mbit/s [5], which cannot compete with existing technologies [4]. However, with arrays from several hundreds to thousands of levers operating in parallel, the data rate for AFM data storage can be increased substantially. We have recently designed, developed, and fabricated a 32×32 (1024) two-dimensional (2D) cantilever array chip for parallel AFM applications. This chip, in conjunction with the 500 Gbit/in^2 storage density in thin polymer films, is the basis of future high-data-rate, terabit storage devices.

2. Thermomechanical AFM data storage

Thermomechanical data storage [1,2,5–7] constitutes a particularly elegant implementation of an AFM storage scheme. Here a resistive cantilever tip, which is in contact with a polymer storage medium, is heated by current pulses. As a result, indentations representing data bits are formed by a combination of applying a local force to the polymer layer and softening it by local heating. Several issues are involved in this operation, including the spatial and temporal localization of the heat deposition as well as the melting and displacement of media to form data bits. We discovered that the tip must be heated to a relatively high temperature ($\sim$400 °C, well above the glass temperature, $T_g \approx 115$ °C, of the polymer) to initiate the indentation process [2]. Hence, heat transfer from the tip to the polymer through the small contact area is poor [8].

Using this technique, data bits of 40 nm diameter have been written [2], as shown in figure 1, into a layered storage medium consisting of a Si substrate covered with a 70 nm thick, crosslinked, hard-baked photoresist (SU-8) buffer layer and a 40 nm thick PMMA film. The writing was performed using a 1 μm thick, 70 μm long, two-legged Si cantilever. The resistive heater region at the tip is formed by heavy-ion implantation of the cantilever legs with the lightly doped tip region masked off. The patterns were written by applying electrical pulses of 2 μs duration to the cantilever tip and repeating the process every 50 μs.

Imaging and reading back of the data is performed in a constant-height, contact AFM operating mode. The tip always is in contact with the medium and acts as a stylus profilometer similar to a standard record player. No feedback is applied to the tip other than a global adjustment of the loading force, which is of the order of a few hundred nanonewtons. The vertical motion of the tip reflecting the surface topography is sensed using an anemometer-style operation of the heater cantilever (see figure 2). For this purpose, the tip platform is heated to approximately 300 °C. As the tip plunges into an indentation in the PMMA film representing a written bit, the distance between the lever arm and the surface is reduced (see figure 2). As a conse-

* Also at IBM Research, Zurich Research Laboratory, CH-8803 Rüschlikon, Switzerland.

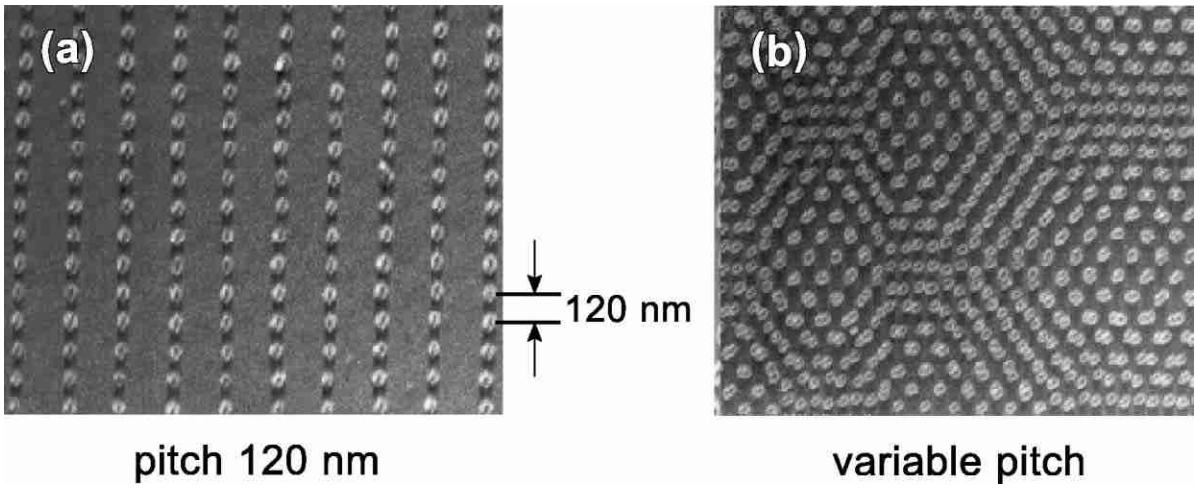

Figure 1. Series of 40 nm data bits written into a 40 nm thick PMMA film: (a) regular bit array with 120 nm pitch and (b) bit pattern with variable pitch. Smallest bit separation is 40 nm corresponding to an areal bit density of ∼400 Gbit/in^2 (adapted from [2]).

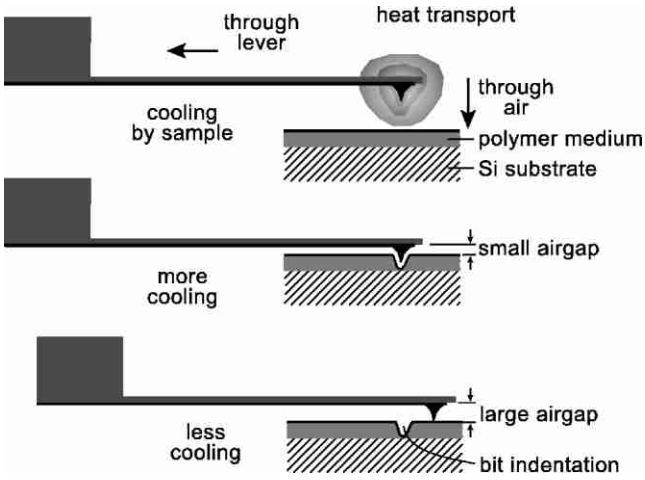

Figure 2. Principle of AFM thermal sensing. The tip of the cantilever is continuously heated by a DC power supply. A bit is sensed via a tiny change of the resistance of the heater stage induced by a modulation of the heat conductance through the air gap as the tip follows the contour of an indentation. From [12], © 1999 IEEE.

quence, a slightly higher fraction of the heat is dissipated to the substrate, thereby lowering the temperature in the heater platform by a small amount. The platform temperature, in turn, is sensed electrically via the thermoresistive effect in the semiconducting heater platform. Under typical operating conditions a resistance variation of the order of $\Delta R/R \approx 10^{-5}$ is obtained per nanometer of lever deflection, translating into one half part per mille total change of the resistance for the sensing of a bit.

In addition to ultra-dense, thermomechanical writing and reading, erasing and rewriting capabilities of the polymer storage media have also been demonstrated. Thermal reflow of a storage field is achieved by heating the media to 150 °C for a few seconds. The smoothness of the reflowed media allowed multiple rewriting of the same storage field [2].

At present, we only have a sketchy empirical understanding of the read/write mechanism. Bit writing, i.e., forming an indentation in the PMMA, depends on several parameters such as scan speed, heating time, loading force, and heating power. So far, no systematic study of the parameter space has been performed, and the numbers quoted in this paper should be understood as typical experimental values. The most prominent feature, however, is the fact that the tip temperature is substantially higher than the glass temperature of the polymer, even in read mode, yet no experimentally detectable damage to the polymer surface occurs, even after repetitive scanning of the same area. Clearly, heat transport through the nanometer-scale tip–polymer contact is extremely poor, which is an important tribological property. In fact, simulations [8] suggest that only a small fraction (of the order of 1%) of the heat generated in the platform is dissipated through the tip.

3. Millipede storage concept

The 2D cantilever array concept, called Millipede, is illustrated in figure 3. A comprehensive description of the concept has been published in [3]. It is based on an "en bloc" x/y scanning of either the array chip or the storage medium. The Millipede concept does not employ individual height control for each lever [9,10], but relies instead on global feedback for the entire chip, which greatly simplifies the system. The tips of 32×32 cantilevers must be simultaneously in contact with the sample at a given loading force. This requires excellent uniformity of tip height, accurate control of level bending, and precise chip alignment with respect to the sample within a cumulative error of less than $\sim$0.2 μm across the entire chip.

The basic Millipede concept entails a time-multiplexing scheme for addressing the array in a row-by-row fashion, similar to the approach used for DRAMs. Furthermore, the storage medium is divided into 32×32 storage subfields with the size of the pitch between two cantilevers, and each cantilever reads and writes only in its own subfield. Hence, for operation of the Millipede, position tolerances of the

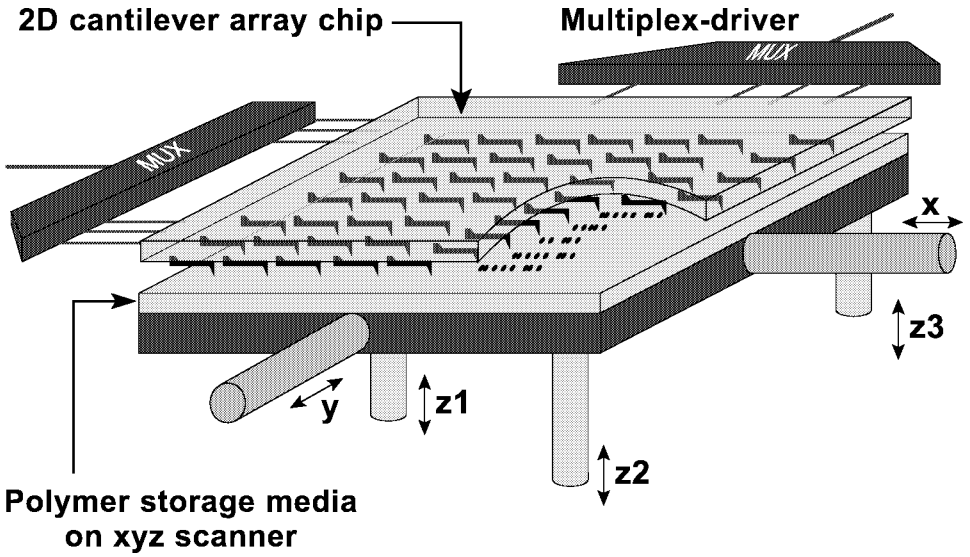

Figure 3. Millipede concept. From [12], © 1999 IEEE.

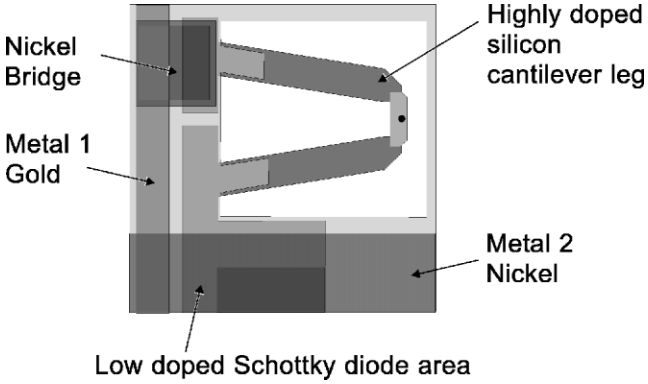

Figure 4. Cantilever cell layout. From [12], © 1999 IEEE.

tips relative to each other are immaterial. The Millipede chip consists of 32×32 sensor cells (figure 4) arranged in a square pattern and interconnected in a crossbar architecture. The cell area and x/y cantilever pitch is 92×92 μm^2, which results in a total array size of less than 3×3 mm^2 for the 1024 cantilevers. The cantilevers are made entirely of silicon for good thermal and mechanical stability. They consist of a heater platform with a tip on top, and legs acting as a mechanical spring and electrical connections (made of highly doped Si) to the heater. On the lever, no metal wiring was used, in order to eliminate electromigration and parasitic z actuation of the lever due to a bimorph effect. The leg resistance, $\sim$400 Ω, is about one order of magnitude smaller than the resistance of the heater platform, $\sim$3 kΩ, in the current design of the chip. This ensures that essentially all electrical power is dissipated in the heater section and only negligible electrical heating occurs in the lever legs. The dimensions of the lever are: 50 μm long, 10 μm wide and 0.5 μm thick legs, and a 5 μm wide, 10 μm long and 0.5 μm thick platform. Such a cantilever has a stiffness of 1 N/m and a resonant frequency of 200 kHz. The time for the cantilever to reach bit-writing temperatures is of the order of 1 μs [11], which should allow multiplexing rates of up to 100 kHz. Figure 5 shows the fabricated chip with the 32×32 array in the center and the electrical wiring connecting the array with the bonding pads. Details of the chip fabrication are provided in [12].

4. Write/read results with the 32×32 array chip

Positioning, alignment, and scanning of the Millipede chip with respect to the storage medium is a crucial issue of the basic Millipede concept shown in figure 1. For this purpose a five-axis, rotation–translation stage was developed that allows the chip to be leveled with respect to the PMMA surface, adjusting the tip loading force by means of precise control of the vertical chip–storage medium distance, and raster-scanning in the x–y direction. The device operates similarly to a loudspeaker using permanent magnets and actuator coils arranged in a compact planar structure [13].

A 3×3 mm^2 silicon substrate spin coated with the SU-8 ($\sim$70 nm)/PMMA ($\sim$50 nm) polymer storage medium served as sample. The sample was attached to the scanning/positioning stage. The parallel alignment of sample and Millipede chip is monitored by four additional cantilever sensors in the corners of the array. The signals from these corner levers are also used to control the forces acting on the Millipede cantilevers while they are in contact with the medium by means of a feedback scheme. The feedback is continuously active during read/write operation while raster-scanning the storage medium at a speed of typically 100 μm/s.

The PC-controlled write/read scheme addresses the 32 cantilevers of one row in parallel. Writing is performed by connecting the addressed row for 20 μs to a high negative voltage (~ -10 V) and simultaneously applying data inputs (0 or 1) to the 32 column lines. This translates into a net data rate of the order of 1 Mbit/s [14]. The data input is a high positive voltage ($\sim +10$ V) for a "1" and ground for

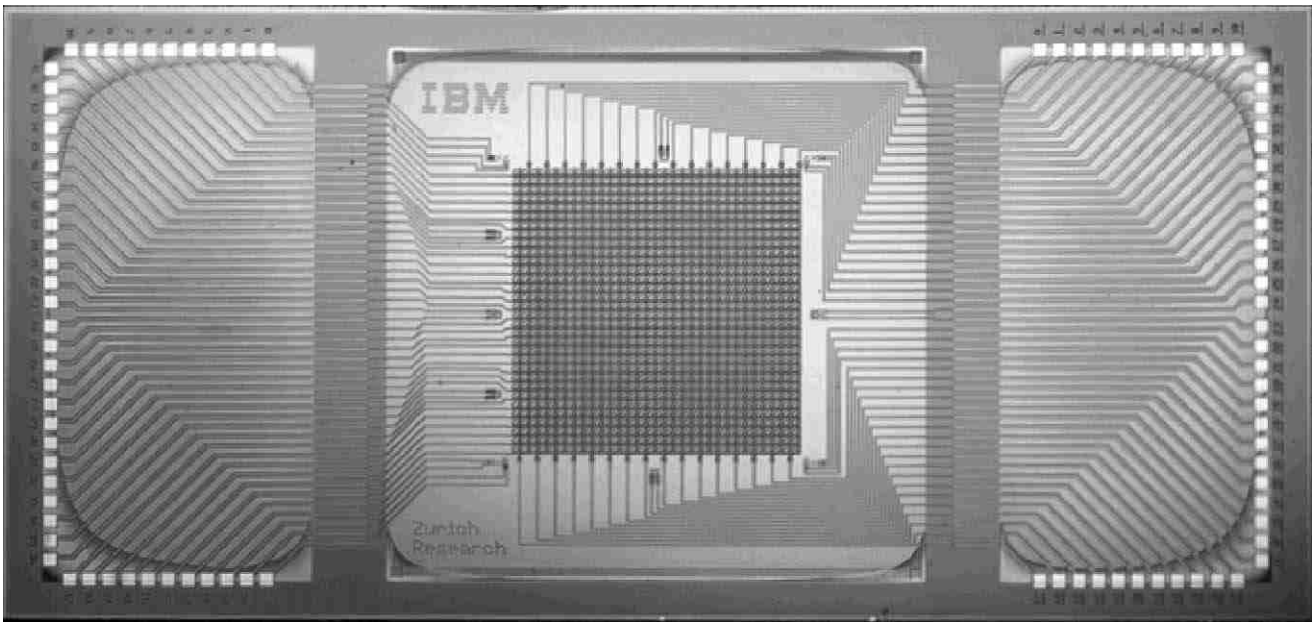

Figure 5. Photograph of the fabricated chip (14×7 mm^2). The 32×32 cantilever array is located at the center and the bond pads are distributed on either side. From [12], © 1999 IEEE.

a "0". This row-enabling and column-addressing scheme supplies a heater current to all cantilevers, but only those levers with high positive voltage generate an indentation ("1"). Those with ground are not hot enough to make an indentation, and thus write a "0". When the scan stage has moved to the next bit position (note that the scan velocity, $\sim$100 μm/s, is constant during reading and writing), the process is repeated, and this is continued until the line scan is finished. In the read process, the selected row line is connected to a moderate negative voltage (~ -5 V), and the column lines are grounded via a protection resistor of about 10 kΩ, which keeps the cantilevers in the selected row warm. During scanning, the voltages across the resistors are measured. If one of the cantilevers falls into a "1" indentation, it cools, thus changing the resistance of the heater platform. This in turn gives rise to a corresponding change of the voltage across the series resistor, which is sensed using a standard analog data acquisition card in the PC. In the experiment, a readout data rate comparable to writing, viz. $\sim$1 Mbit/s, was achieved.

Scanning electron microscopy (SEM) micrographs and AFM images recorded with the Millipede chip operating in the read mode are shown in figure 6. Figure 6(a) shows an SEM image of a large area of the polymer medium, in which many small bright spots indicate the location of storage fields with data written by the corresponding cantilevers. The data written consisted of an IBM logo composed of indentations ("1") and clear separations ("0"). Figure 6(b) shows magnified images of two storage fields. The dots are about 50 nm in diameter, which results in areal densities of 100–200 Gb/in^2. A first successful attempt demonstrating the readback of stored data using thermomechanical sensing is shown in figure 6(c). Here, written patterns consisted of the IBM logo plus a number indicating the column line corresponding to the lever. The areal density is similar to that in figure 6(b).

5. Lifetime studies

Despite the experimental expertise accumulated in the operation of the Millipede chip we have only little understanding of the deformation mechanics in the thin PMMA storage layer. The problem is exacerbated by the fact that macroscopic viscoelastic parameters of bulk material cannot be faithfully extrapolated to nanometer dimensions, which are relevant in our case. Yet, design of optimum writing schemes and, even more importantly, predicting the long-term stability of written data bits requires a thorough underpinning of the critical issues on a scientific basis.

As a starting point we investigated the annealing of periodic artificial patterns, which were fabricated in the PMMA storage medium and which had dimensions relevant to the size of a typical data bit, i.e., the order of a few tens of a nanometer, using a light-scattering technique. The setup is shown schematically in figure 7. The sample is illuminated by a laser beam at an incident angle of $\sim$75°. The intensity of the light beam refracted by the periodic pattern is measured by means of a photodiode. The scattering angle of the refracted beam is determined by the condition that the in-plane scattering vector $\boldsymbol{q} = \boldsymbol{k}_\mathrm{i} - \boldsymbol{k}_\mathrm{f}$ must be a reciprocal lattice vector of the pattern, where $\boldsymbol{k}_{\mathrm{i,f}}$ denote the projected wave vectors of the incident and refracted beam, respectively. The sample is mounted on a temperature-controlled heater stage. In the experiment the sample temperature is rapidly (within 50 s) raised from room temperature to a fixed temperature T greater than the glass temperature, T_g, of the PMMA film, and the intensity of the refracted light beam is measured as a function of time.

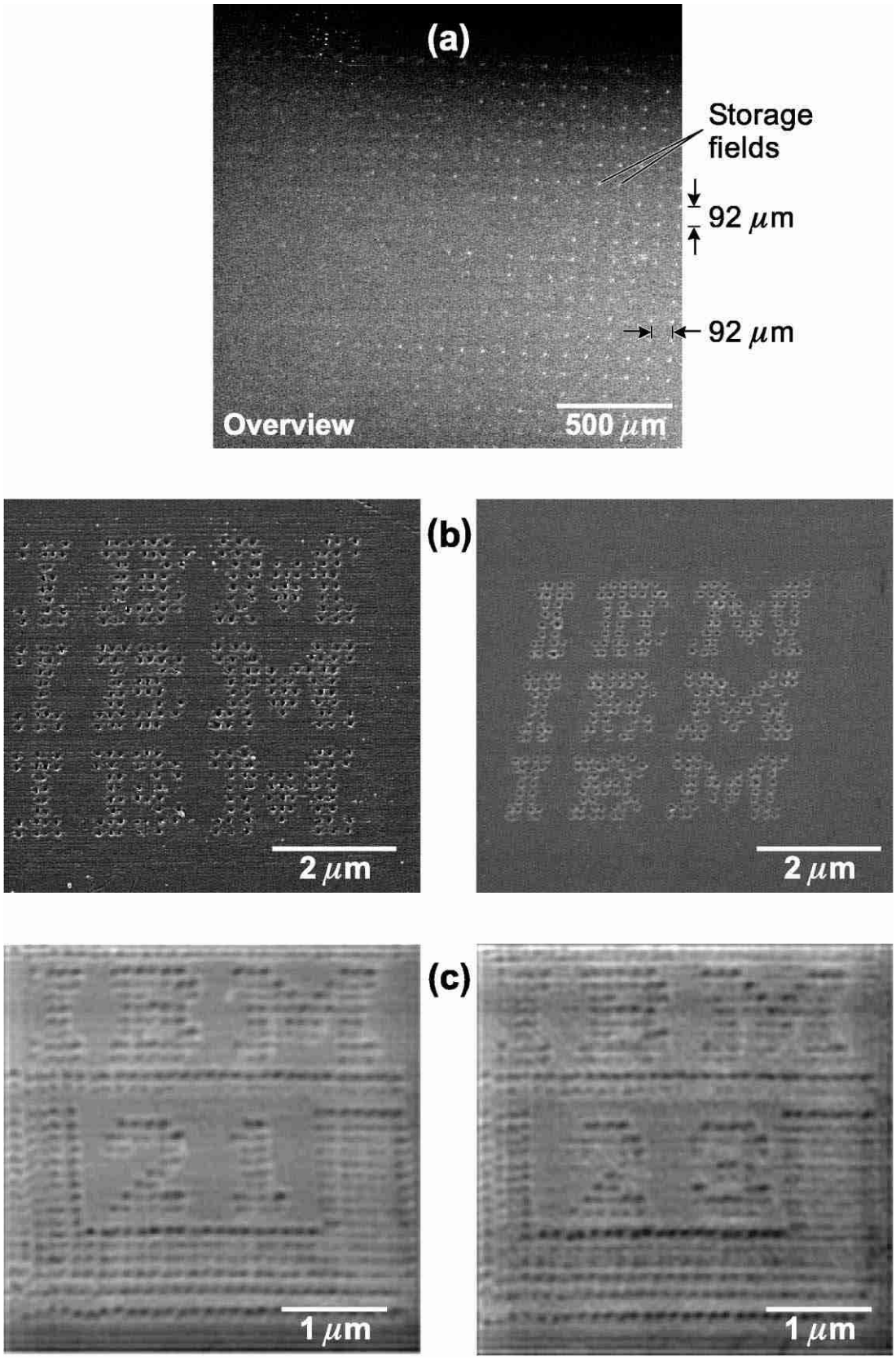

Figure 6. Images of Millipede write/read results. (a) Large-scale SEM image of many storage fields. Bright dots represent data written by individual levers of the Millipede chip. (b) Magnified views of two individual storage fields with IBM logo represented by bit indentations/separations equivalent to a storage density of 100–200 Gbit/in^2 (50 nm thick PMMA medium). (c) Thermomechanical readback signals of two storage fields demonstrating an areal density similar to those in (b). From [3].

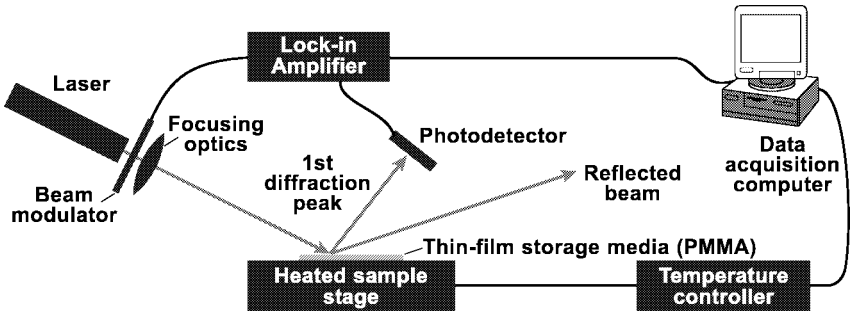

Figure 7. Sketch of the experimental setup.

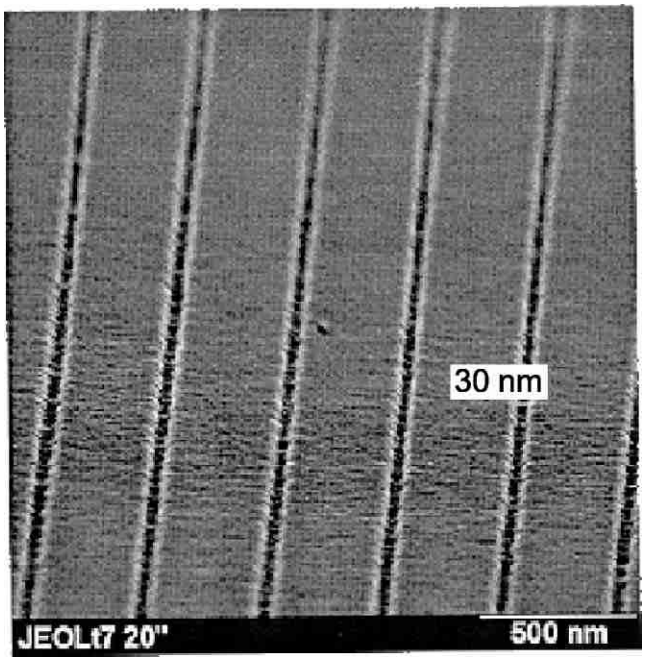

Figure 8. SEM micrograph showing a line grating with a pitch of 370 nm written into a 70 nm thick PMMA film. The width of the lines is 30 nm.

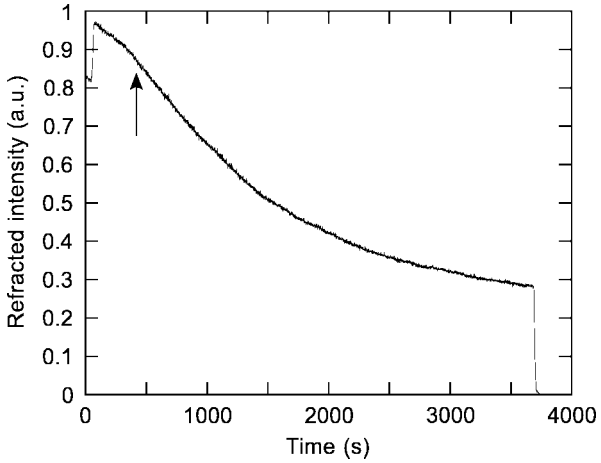

Figure 9. Refracted intensity versus time recorded at a temperature of 125 °C. Note the discontinuity in the slope of the curve at the position marked by the arrow. The steep intensity drop at $t = 3700$ s was induced by a rapid anneal at 180 °C, which serves as a reference measurement of the background intensity.

Figure 8 shows an SEM micrograph of one representative sample investigated. The regular line grating consisting of trenches that penetrate the entire PMMA film was produced by means of electron-beam lithography using a standard SEM as exposure tool. The pitch of the grating was 370 nm and it covered a sample area of $500 \times 500\ \mu\text{m}^2$. With a wavelength of the illuminating HeNe laser beam of 632 nm one obtains one refraction spot at a scattering angle of $\sim -40°$. Samples with a width of the trenches of $w = 30$ nm were investigated. The thickness of the PMMA film was 70 nm spin-coated on an SU8-epoxy buffer layer similar to the samples used in the Millipede experiments.

Figure 9 shows a typical example of an intensity-versus-time curve for such samples. Here, $w = 30$ nm and the sample was heated to a final temperature of $T = 125\,°\text{C}$. The heating was started at $t = 0$. As the temperature reached a value of $115 \pm 2\,°\text{C}$ at $t \approx 50$ s an abrupt increase of the refracted intensity by $\sim$10% was consistently observed. We identify this feature with a relaxation of the polymer pattern, i.e., a rounding-off of the edges, which in turn increases the scattering volume, associated with the glass transition. The final sample temperature is reached about 10 s later. During the first $\sim$400 s the intensity decays fairly linearly with time. At the point indicated by the arrow a distinct transition to a different relaxation mode occurs, characterized by a discontinuity of the slope of the intensity curve, which subsequently decays gradually with time at an increasingly lower rate. At $t = 3700$ s the temperature was abruptly increased to 180 °C, at which the pattern anneals almost instantaneously. We use this for the *in situ* calibration of our background scattering intensity.

The intensity curves measured at different annealing temperatures of up to $\sim$130 °C all exhibited the same characteristic features described above. However, the time constants involved depend strongly on temperature. The self-similarity of the curves indicates scaling behavior. Indeed we find that the various curves can be superimposed almost perfectly by rescaling the time axis using the transformation

$$\tilde{t} = t\left(\frac{T - T_\text{g}}{T_\text{g}}\right)^{-4.7}, \qquad (1)$$

where $T_\text{g} = 115\,°\text{C}$ is the glass temperature. The results are summarized in figure 10(a), which shows the intensity measured at $T = 120, 125$, and 130 °C versus rescaled time on a log–log scale. In particular, we find that after an initial

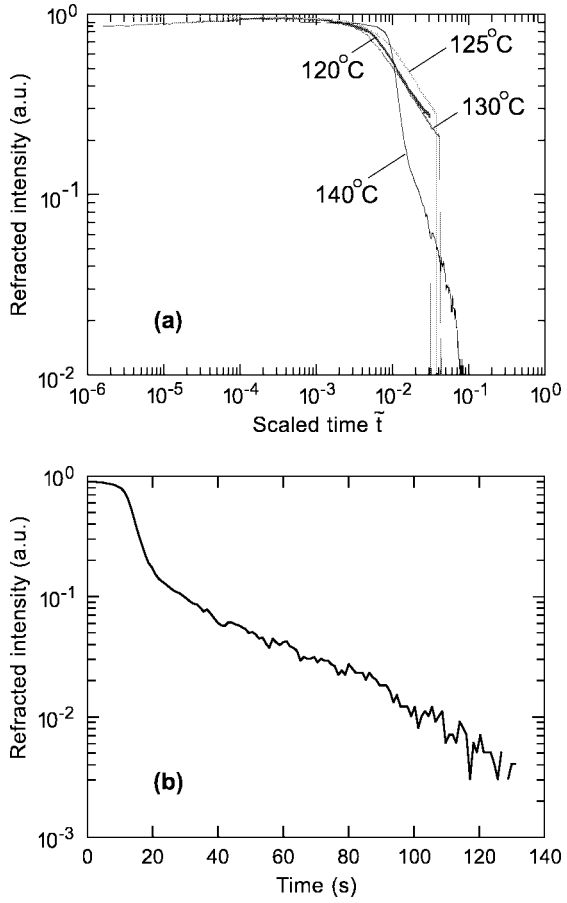

Figure 10. (a) Refracted intensity versus rescaled time $\tilde{t}$, see equation (1), plotted on a log–log scale. Note that the curves recorded at a temperature of less than 140 °C superimpose almost perfectly. The slope of the decay for $\tilde{t} > 0.004$ corresponds to an exponent of 1.56 ± 0.06. (b) Refracted intensity recorded at a temperature of 140 °C plotted on a log–lin scale. Note that, in contrast to the data at lower temperature, the intensity decays exponentially with time.

dwell time of the order of $\tilde{t}_0 \approx 0.004$ the intensity decreases as a power law with an exponent of 1.56 ± 0.06. The other intriguing feature in figure 10(a) is the intensity curve measured at 140 °C, which clearly violates scaling. At this temperature the intensity drops quasi-instantaneously by almost one order of magnitude as soon as the final temperature is reached and, in contrast to the lower temperature curves, the subsequent relaxation is exponential, see figure 10(b).

In order to rationalize the results we recall that the scattered light intensity is proportional to the dynamic structure factor $g(\boldsymbol{q}, t)$, which is the spatial Fourier transform of the density correlation function $c^2(r, t) = \langle \rho(r, t)\rho(0, 0)\rangle$. Hence, our experiment probes the relaxation of the sinusoidal density modulation with wave vector $\boldsymbol{q}$, which is associated with the pattern.

We first discuss the data for $T_g < T < 140\,°C$. Note that in the process of making the line grating, material was actually removed. Thus, restoring a flat surface is eventually a nonlocal process involving material flow on a length scale of the periodicity of the grating. However, initially we may think that the trenches are filled by local reflow of material from the edges. Owing to mass conservation, the trenches must widen accordingly. From a scattering point of view, we expect that the intensity does not change appreciably during this first phase because the scattering volume remains essentially constant as long as the width of the trenches is small compared to the grating period. As the trench width becomes comparable to the grating period, the trenches no longer grow independently from one another. Instead, we are reminded now of a pattern that has evolved into a cosine grating. From here on, equilibration reduces the scattering volume, which is reflected by the transition to a steeper power-law decay of the scattering amplitude for $\tilde{t} > 0.004$. The fact that the amplitude decays with time at some power law rather than exponentially is a clear sign for nonstandard viscous flow, reflecting the highly constrained phase space available in the entangled polymer medium. At sufficiently high temperatures $T \gtrsim 140\,°C$ the polymer chains acquire enough mobility to equilibrate density fluctuations by cooperative diffusion as manifested by the exponential decay of the scattered intensity. Here, the kinetics are equivalent to standard viscous flow, as in a simple liquid. Although the scattering experiment does not answer questions directly related to bit lifetimes, the experiment provides us with important clues for understanding the flow dynamics of thin polymer films, which is a central issue in bit writing and erasing. In particular, we have identified a transition from frustrated diffusion characterized by scaling behavior below 140 °C to simple liquid-like behavior above 140 °C.

6. Conclusions and outlook

The Millipede AFM storage concept provides a possible roadmap towards future terabit storage systems. Storage densities of up to 500 Gbit/in^2 have been realized by thermomechanical writing and readback in thin (PMMA) film media. We have fabricated and successfully operated the densest and largest 2D AFM cantilever array chip with 32×32 (1024) cantilevers packed into an area of only 3×3 mm^2.

Data rates of the order of 1 Mbit/s have been demonstrated using the Millipede concept. This data rate is imposed by constraints of the currently used experimental electronics and does not represent a fundamental limit of the Millipede concept. In fact, with the current chip, data rates approaching 500 Mbit/s are feasible [11], which is of the order of magnitude of state-of-the-art hard-disk drives. It can be shown that the data rate can be pushed to an impressive 10 Gbit/s merely by reducing lever dimensions by a factor of 2 [11]. The Millipede project is still in the research phase with many important questions lacking firm answers. By its very design, the project constitutes a nanotribology testing ground for a multi-asperity contact between oxidized silicon tips and a polymer surface. The experimental observations indicate so far that neither tip wear nor accidental modification of the PMMA surface

is a critical issue as long as the loading force per asperity is less than 1 μN. This qualitative statement must still be quantified by much more detailed experimental studies, which are currently being pursued. Furthermore, we have demonstrated that extremely large temperature gradients of the order of hundreds of degrees C per micrometer can be maintained across nanometer-scale asperity contacts. Another critical issue is bit lifetime. So far, we see no degradation effects in samples stored at room temperature. In this context, we have performed a light-scattering study of the annealing properties of nanometer-scale patterns in thin PMMA films, which revealed an unexpectedly rich, scale-related phenomonology.

We expect that more surprises will come to light as pertinent technological issues are subjected to scientific scrutiny.

Acknowledgement

The authors gratefully acknowledge the technical contributions of, stimulating discussions with, and the encouraging support of R. Beyeler, G. Genolet, R. Germann, S. Granick, T.W. Kenny, U. Landman, and P.F. Seidler.

References

[1] H.J. Mamin, B.D. Terris, L.S. Fan, S. Hoen, R.C. Barrett and D. Rugar, IBM J. Res. Develop. 39 (1995) 681.
[2] G. Binnig, M. Despont, U. Drechsler, W. Häberle, M. Lutwyche, P. Vettiger, H.J. Mamin, B.W. Chui and T.W. Kenny, Appl. Phys. Lett. 74 (1999) 1329.
[3] P. Vettiger, M. Despont, U. Drechsler, U. Dürig, W. Häberle, M.I. Lutwyche, H.E. Rothuizen, R. Stutz, R. Widmer and G.K. Binnig, IBM J. Res. Develop. 44 (2000) 323.
[4] E. Grochowski and R.F. Hoyt, IEEE Trans. Magn. 32 (1996) 1850.
[5] R.P. Ried, H.J. Mamin, B.D. Terris, L.S. Fan and D. Rugar, J. Microelectromech. Syst. 6 (1997) 294.
[6] B.W. Chui, H.J. Mamin, B.D. Terris, T.D. Stowe, D. Rugar and T.W. Kenny, Appl. Phys. Lett. 69 (1996) 2767.
[7] B.W. Chui, T.D. Stowe, Y.S. Ju, K.E. Goodson, T.W. Kenny, H.J. Mamin, B.D. Terris, R.P. Ried and D. Rugar, J. Microelectromech. Syst. 7 (1998) 69.
[8] W.P. King and K.E. Goodson, in: *Microelectromechanical Systems (MEMS) 1999*, Vol. 1, eds. A.P. Lee, L. Lin, F.K. Forster, Y.C. Young, K. Goodson and R.S. Keynton (ASME Press, New York, 1999) pp. 583–588.
[9] N.C. MacDonald, in: *Digest of Technical Papers, 7th Int. Conf. Solid-State Sensors and Actuators*, Yokohama, Japan, 7–10 June 1993, pp. 8–12.
[10] S.C. Minne, G. Yaralioglu, S.R. Manalis, J.D. Adams, A. Atalar and C.F. Quate, Appl. Phys. Lett. 72 (1998) 2340.
[11] W.P. King, T.W. Kenny, K.E. Goodson, G. Cross, M. Despont, U. Drechsler, U. Dürig, W. Häberle, M. Lutwyche, H. Rothuizen, R. Stutz, R. Widmer, G.K. Binnig and P. Vettiger, in: *Proc. 2000 Solid-State Sensor and Actuator Workshop*, Hilton Head, SC, 4–8 June 2000 (Transducers Research Foundation, Cleveland, OH), in press.
[12] M. Despont, J. Brugger, U. Drechsler, U. Dürig, W. Häberle, M. Lutwyche, H. Rothuizen, R. Stutz, R. Widmer, G. Binnig, H. Rohrer and P. Vettiger, in: *IEEE Int. Micro Electro Mechanical Systems Technical Digest 1999 (MEMS 99)*, Orlando, FL, January 1999 (IEEE, Piscataway, 1999) pp. 564–569.
[13] M. Lutwyche, U. Drechsler, W. Häberle, H. Rothuizen, R. Widmer and P. Vettiger, in: *Magnetic Materials, Processes, and Devices. Application to Storage and Micromechanical Systems (MEMS)*, Vol. 98-20, eds. L.T. Romankiw, S. Krongelb and C.H. Ahn (Electrochemical Society, Pennington, 1999) pp. 423–433.
[14] M.I. Lutwyche, G. Cross, M. Despont, U. Drechsler, U. Dürig, W. Häberle, H. Rothuizem, R. Stutz, R. Widmer, G.K. Binnig and P. Vettiger, in: *Digest of Technical Papers IEEE Int. Solid-State Circuits Conf. ISSCC 2000*, San Francisco, CA (IEEE, Piscataway, 2000) pp. 802–803.